*Geophys. J. Int.* (2006) **164,** 312–318 doi: 10.1111/j.1365-246X.2006.02848.x



# Identifying the origin of the magnetic directional anomalies recorded in the Datong loess profile, northeastern Chinese loess plateau

Rixiang Zhu,[1] Qingsong Liu,[1,2]* Yongxin Pan,[1] Chenglong Deng[1] and Jimin Sun[1]

[1]*Palaeomagnetism and Geochronology Laboratory (SKL-LE), Institute of Geology and Geophysics, Chinese Academy of Sciences, Beijing* 100029*, China*
[2]*Department of Earth Sciences, University of California at Santa Cruz, CA* 95064*, USA*

Accepted 2005 October 17. Received 2005 August 15; in original form 2005 April 11

## SUMMARY

To better understand the origin of short-term features of palaeomagnetic signals recorded by the Chinese loess, detailed palaeomagnetic and magnetic fabric studies were conducted on a loess profile at Datong, the northeastern margin of the loess plateau, which is characterized by both high sedimentation rate (∼18 cm ka$^{-1}$) and variations of sedimentary environments. It appears that the magnetic fabrics, specifically the inclination of the maximum magnetic susceptibility principal axis (K1-Inc), are robust means to identify the deposition environments. Our results (<∼74 ka) record four palaeodirectional anomalies (referred as A–D). Among them, anomaly C with relatively normal fabrics can be correlated to the Laschamp (∼40 ka) excursion. In contrast, anomalies A, B and D accompanying with K1-Inc anomalies, are interpreted to be caused by post-depositional disturbances. The new results improve our understanding of the origins of the natural remanent magnetization recorded by the Chinese loess.

**Key words:** Chinese loess, geomagnetic excursions, magnetic fabrics.

## 1 INTRODUCTION

The Chinese loess/palaeosol sequence is one of the most important terrestrial records to document palaeomagnetic signals. Detailed magnetostratigraphy and rock magnetic studies have been well conducted over the last two decades (Heller & Evans 1995; Maher 1998; Evans & Heller 2001). The palaeomagnetic studies on the Chinese loess can be classified generally as two categories: one focusing on magnetic reversals (Rolph *et al.* 1989; Sun *et al.* 1993; Zhu *et al.* 1993, 1994a; Spassov *et al.* 2003); and the other on geomagnetic excursions (Zhu *et al.* 1994b; Zheng *et al.* 1995; Fang *et al.* 1997; Zhu *et al.* 1999; Pan *et al.* 2002).

Heller & Liu (1982) investigated thermal demagnetization behaviour of the natural remanent magnetization (NRM) carried by the loess samples at Luochuan, central loess plateau, and claimed that the characteristic remanent magnetization (ChRM) isolated at high-temperature intervals was dominated by the chemical remanent magnetization (CRM) carried by haematite. However, later studies revealed that the aeolian coarse-grained magnetite, responsible for the detrital remanent magnetization (DRM), is the dominant magnetic carrier for the loess deposits, which was subsequently overprinted by the CRM and viscous remanent magnetization (VRM) carried by fine-grained pedogenic maghemite particles (e.g. Zhu *et al.* 1994a,b).

Despite these previous studies, the acquisition history and the fidelity of the loess NRM still appear to be an open question. Zhu *et al.* (1994b) showed that the loess units record fast secondary reversals within a complete reversal. Pan *et al.* (2002) documented that several excursions since the Matuyama/Brunhes (M/B) reversal can be identified in the Chinese loess/palaeosol sequences. Yang *et al.* (2004) revealed two distinct geomagnetic excursions in the Late Matuyama Chron from a loess–palaeosol sequence at Baoji, southern Chinese loess plateau, which are probably correlated with the Kamikatsura and Santa Rosa excursions, respectively. All of these features suggest that the Chinese loess/palaeosol sequences can record short-term features of palaeomagnetic signals, indicating weak effects of smoothing caused by the 'lock-in' processes. In contrast, Zhou & Shackleton (1999) pointed out that the M/B geomagnetic reversal recorded in the Chinese loess (glacial deposits) disagrees with most of the global marine sediments records, in which the reversal occurs in interglacial sediments. Assuming a palaeoclimatic consistency between the stratigraphy of loess and marine sediments, they proposed that the remanence-carrying grains did not block in the reversed polarity until some time after the reversal. Due to a slow NRM acquisition process, the NRM records in the Chinese loess may have a 'lock-in' depth ranging from a few tens of cm to 300 cm, corresponding to a time delay of about 30 000 yr. Therefore, the NRM records in the Chinese loess may be uncertain (Zhou & Shackleton 1999). Zhu *et al.* (1998a) argued that there could exist a phase lag between the climate records in the loess and marine

*Now at: School of Ocean & Earth Science, University of Southampton, National Oceanography Centre, Southampton, European Way, Southampton SO14 3ZH, UK. E-mail: qsl@noc.soton.ac.uk.

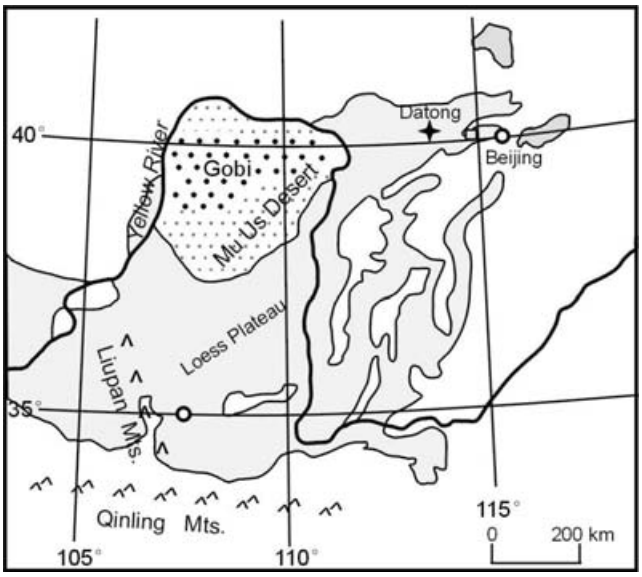


**Figure 1.** Schematic map showing the Chinese loess plateau and the sampling site (Datong).

sediments caused by local climatic change. More recently, Spassov *et al.* (2003) designed a 'lock-in' model to reconcile the contradiction between the downward shifting of the palaeomagnetic records and keeping the short-term features.

The complexity of the loess NRM, especially for the short-term features, can also be caused by post-depositional disturbances during pedogenesis. Unlike lake and marine sediments, loess deposits are exposed in air. If sedimentation rate is low, reworking effects on the surface deposits will be strong. This has been attributed to one of the most important factors for the inconsistency of the Blake event recorded in different regions of the loess plateau (Zhu *et al.* 1998b).

The ambiguities of the palaeomagnetic signals recorded by the Chinese loess can be partly solved by interprofile comparisons. Most of the previous studies focused on results from the western and central loess plateau. Up to now, no attempts have been made to the northeastern margin, which is supposed to be characterized by high disturbance and high sedimentation rates (Liu 1958). Therefore, this study aims to construct a detailed palaeomagnetic study on such a characteristic profile from Datong (113°42′E, 40°12′N), the northeastern margin of the loess plateau (Fig. 1). Anisotropy of magnetic susceptibility (AMS) was further applied to identify the origin of these cryptic short-term palaeodirectional anomalies.

## 2 GEOLOGICAL SETTING AND SAMPLING

The Datong section consists of ∼16 m of Late Pleistocene loess–palaeosol sequence interbedded with three fluvial layers. The profile is situated in the Datong Basin, which is a west–east elongated basin with an area of 30 × 150 km$^2$ and an altitude of ∼1000 m. Samples were collected along a well-exposed gully wall after removing a half-metre thickness of exterior sediments, to eliminate weathered material and disturbance due to vegetation. Large block samples, with approximately 10 cm sides and 30 cm height, were cut and orientated *in situ* using a magnetic compass. Cubic specimens (8 cm$^3$) were prepared from these blocks in the laboratory.

## 3 EXPERIMENTS

### 3.1 OSL dating measurements

The chronological framework of this profile is constructed based on age controls by optically stimulated luminescence (OSL) dating techniques (Huntley *et al.* 1985; Hütt *et al.* 1988). First, polymineral fine-grained fractions (4–11 $\mu$m) were extracted from the sediments. For detailed descriptions for preparing samples, measurements of luminescence and age calculations, refer to Lang *et al.* (1996).

OSL measurements were made using a Daybreakl l00 automated OSL/TL reader equipped with a combined blue light emitting diode (LED) and IR solid-state laser diode OSL unit. The $^{90}$Sr $\beta$ source delivers a dose rate of 3960 mGy min$^{-1}$.

### 3.2 Magnetic measurements

Temperature-dependent susceptibility ($\kappa$-T) curves were measured using a KLY-3 Kappabridge equipped with a CS-3 high-temperature furnace (Agico Ltd., Brno) in an argon atmosphere. The low- and high-frequency magnetic susceptibility was measured with a dual-frequency Bartington Susceptometer at 470 and 4700 Hz, respectively. The parameter $\kappa_{fd}$ per cent was defined as 100 per cent*$(\kappa_{470\,\mathrm{Hz}} - \kappa_{4700\,\mathrm{Hz}})/\kappa_{470\,\mathrm{Hz}}$.

The remanence measurements were made using a 2G Enterprises Model 760-R cryogenic magnetometer installed in a magnetically shielded space (<300 nT). All specimens were subjected to stepwise alternating field (AF) demagnetization with field steps of 5–10 mT. Parallel specimens were also subjected to thermal demagnetization with temperature steps of 25–50°C. The ChRM from each specimen after 200°C/250°C thermal or 10 mT/15 mT AF demagnetization was determined using a least-squares method (Kirschvink 1980).

AMS of all specimens was measured using a KLY-3s Kappa bridge (Agico Ltd., Brno) with an automated specimen handling system. Each specimen was rotated through three orthogonal planes. The susceptibility ellipsoid was calculated by least-squares method (Jelinek 1977). In this study, the inclinations of the maximum (K1) and minimum (K3) principal susceptibility axis were used as one of the criteria for the fidelity of the loess ChRM.

## 4 RESULTS

The depth plots of $\kappa$ and $\kappa_{fd}$ per cent are illustrated in Fig. 2. Due to the existence of the several fluvial sand layers, which also exhibit susceptibility peaks, the pedostratigraphy is determined mainly based on $\kappa_{fd}$ per cent. The susceptibility carried by coarse-grained magnetite in these sand layers is nearly frequency independent. Therefore, $\kappa_{fd}$ per cent can successfully filter out their effects. The OSL ages are also marked in Fig. 2(b). Based on the OSL dating results, the uppermost soil (S0) has an age of Holocene, the thick loess bed with interbedded three thin fluvial layers is labelled L1 accumulated during the last glacial period, whereas the lowest soil (S1) was developed during the last interglaciation. Thus, S0, L1 and S1 correspond to marine oxygen isotope stages (MIS) 1, 2–4 and 5, respectively. The boundaries between 1 and 2 (∼12 ka), and 4 and 5 (∼74 ka), are at ∼2.5 and 14.1 m, respectively.

The temperature dependence of magnetic susceptibility curves for representative loess, palaeosol and sand specimens are shown in Fig. 3. The $\kappa$-T curves for loess and palaeosol specimens resemble those from other regions of the loess plateau (Deng *et al.* 2004; Liu *et al.* 2005a). For example, the susceptibility increases before ∼300°C are due to the gradual

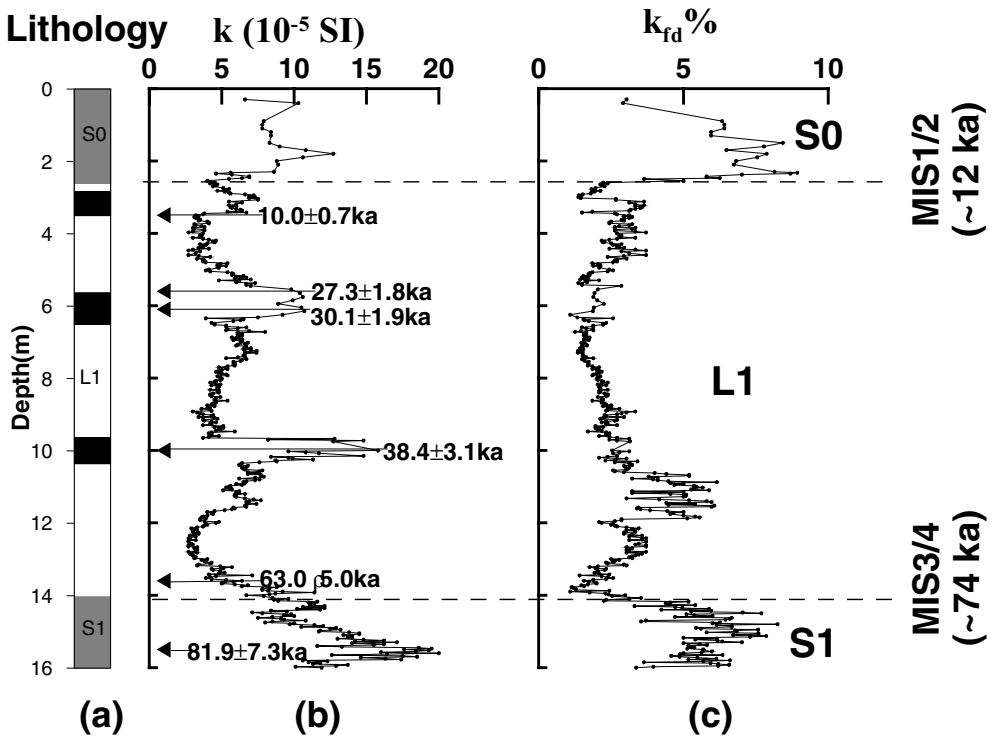


**Figure 2.** Stratigraphy (a) and depth plots of magnetic susceptibility (b) and frequency dependence of magnetic susceptibility (c). Arrows and the associated numbers in (b) are OSL age controls. The two dashed lines mark the boundary of MIS1/2 and MIS3/4, respectively. The black bars in (a) mark the fluvial sand layers.

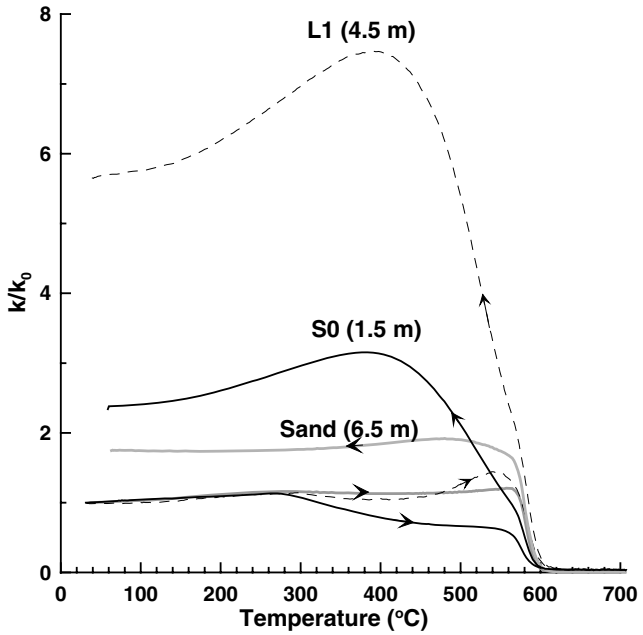


**Figure 3.** Temperature dependence of normalized magnetic susceptibility for the representative specimens of palaeosol at 1.5 m, loess at 4.5 m and fluvial sand at 6.5 m. The thick and dashed lines represent the warming and cooling curves, respectively. Arrows show the heating and cooling processes.

unblocking of SD particles. The susceptibility loss between ∼300 and 450°C, caused by the transformation from pedogenic superparamagnetic maghemite particles to haematite (Liu *et al.* 2005a), increases from loess to palaeosol specimens. The susceptibility peak above 500°C for the loess specimen is due to the neoformation of ferrimagnetic particles during heating. Overall, the loess and sand specimens are dominated by magnetite. In contrast, the palaeosol specimens contain a mixture of magnetite and maghemite. There is a clear trend that the amount of maghemite increases from sand to loess and then to palaeosol based on the susceptibility drop between 300–450°C of the $\kappa$-T curves (Fig. 3). Moreover, the relatively flat pattern of the $\kappa$-T curve for the sand specimens indicates that the magnetite particles are in large pseudo-single domain or multidomain-like grain size region.

The cooling curves for all three samples were highly enhanced, but with different rates. The maximum susceptibility of the cooling curves for the loess and palaeosol samples are at ∼380 and 400°C, respectively, which correspond to the unblocking temperatures of the newly formed SD magnetite particles during heating (Liu *et al.* 2005a). These features also resemble the results from the western loess plateau. In contrast, the sand sample exhibits different features that there are no apparent SD particles (with unblocking temperatures above the room temperature) formed during the thermal treatments as suggested by the lack of the dominant susceptibility peaks around 400°C.

The demagnetization of the NRM spectra for representative specimens is summarized in Fig. 4. For the AF demagnetization, the Zijderveld plots (Zijderveld 1967) do not tend towards the origin, but with stable intensity levels remaining at fields above 30 mT. Such a high-coercivity component has been attributed mostly to the partially oxidized aeolian coarse-grained magnetite (Dunlop *et al.* 2004; Liu *et al.* 2003). In contrast, thermal treatments can efficiently demagnetize the remanences below 580°C for loess, palaeosol and sand specimens. As shown by the representative demagnetization diagrams in Fig. 4, the majority of specimens are characterized by a stable component of magnetization that is isolated after an AF

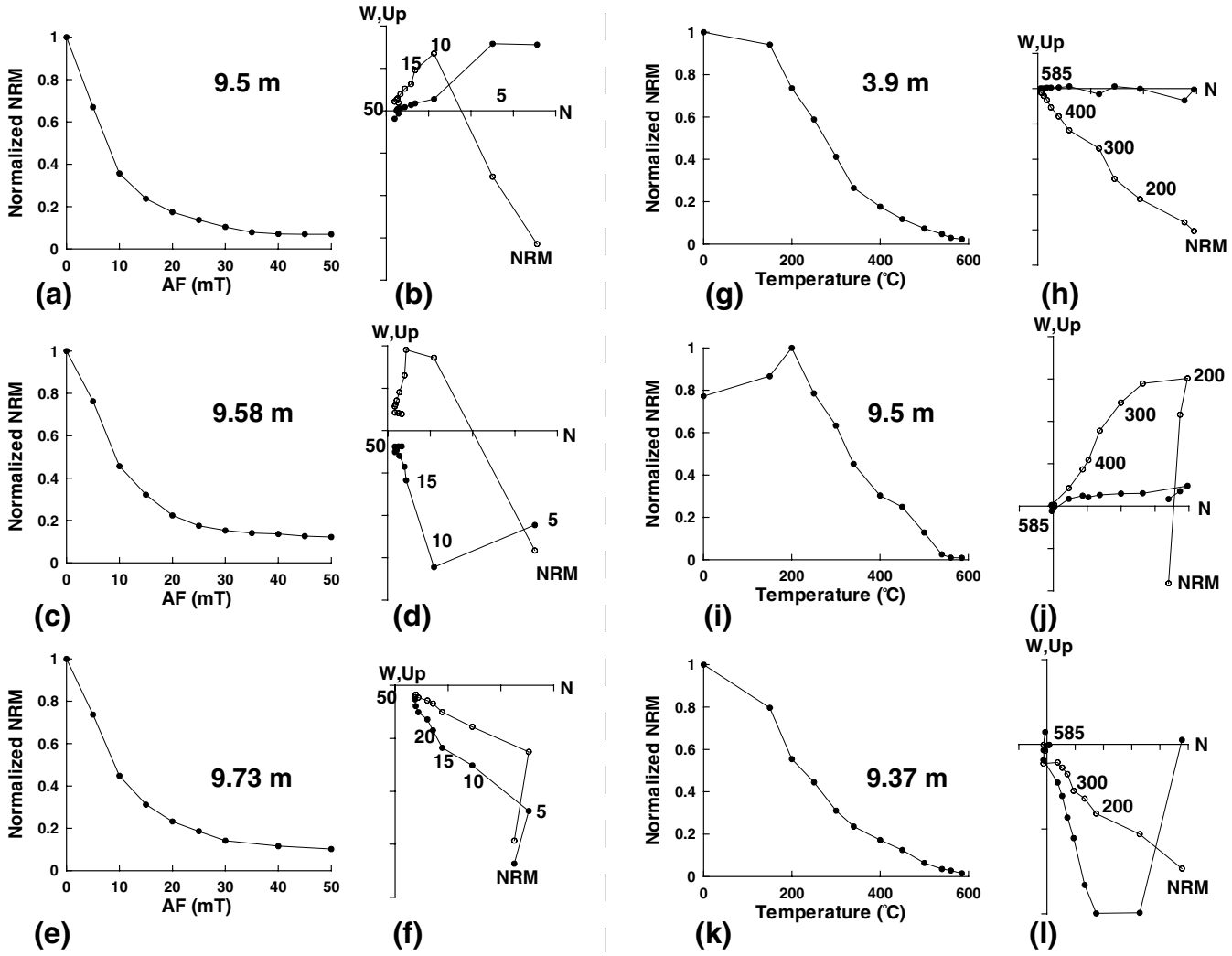


**Figure 4.** AF (a–f) and thermal (g–l) demagnetization spectra and Zijderveld plots of representative specimens. Numbers in (b), (d) and (f) are the applied alternating fields, and numbers in (h), (j) and (l) are temperatures.

demagnetization at 10–15 mT or a thermal demagnetization above 200°C/250°C. The ChRM vector directions yield virtual geomagnetic pole (VGP) latitudes that were subsequently used to define the succession of magnetic polarities at Datong (Fig. 5). The MAD values are generally less than 10°. All together, four directional anomalies (hereafter referred to A-D) were identified. Because the coarse-grained magnetite controls the ChRM isolated by both AF and thermal demagnetizations, these two demagnetization methods basically yield consistent results as shown in Figs 4 and 5, partly indicating that our demagnetization results are reliable. However, it should be noted that thermal demagnetization provides more reliable ChRM direction than the AF demagnetization, therefore is more suitable for the remanence cleaning for loess–palaeosols from the northeastern margin of Chinese loess plateau.

The depth plots of the four palaeomagnetic anomalies and the inclinations of K1 and K3 are shown in Figs 5(c)–(g). The palaeoenvironmental significances of the magnetic fabrics carried by the Chinese loess have been well interpreted by Zhu *et al.* (2004) and Liu *et al.* (2005b). The primary fabrics of loess–fluvial sequences are acquired during its accumulation. Although all minerals (including dia-, para-, and ferri-magnetic) contribute to AMS, the dominant magnetic carriers of the loess magnetic susceptibility are strongly ferrimagnetic phases. Specially, the hysteresis loop (not shown) for a representative fluvial sand sample shows that the contributions from paramagnetic minerals are negligible. Because the magnetic assemblage of Chinese loess sequences consist of aeolian coarse-grained magnetite and pedogenically produced fine-grained maghemite, the measured AMS is, therefore, also the sum of the primary oblate ellipsoids carried by aeolian magnetite and pedogenically produced secondary inverse prolate or oblate ellipsoids (Zhu *et al.* 2004; Liu *et al.* 2005b). Because of the ferrimagnetic phase dominates the magnetic fabrics, the remanence directions are related to the AMS and the fabrics can be used for detection of the physical disturbance after deposition. Among all magnetic fabric parameters, K1-Inc and K3-Inc have been used to check the effects of the post-depositional disturbances (e.g. Zhu *et al.* 1999). Fig. 5 shows that for most specimens, K1 is confined within the bedding plane, indicating a normal oblate fabric. However, anomalies A, B and C coincide with abnormal K1-Inc and K3-Inc.

The depth plots of the degree of anisotropy ($P \equiv$ K1/K3) are shown in Fig. 5(h). Liu *et al.* (1988) found that redeposited loess has a higher degree of anisotropy ($1.032 \leq P \equiv K_{\max}/K_{\min} \leq 1.064$) than wind-blown deposits ($1.002 \leq P \leq 1.032$). Zhu *et al.* (2004) revealed that P is strongly related to the degree of pedogenesis that palaeosols

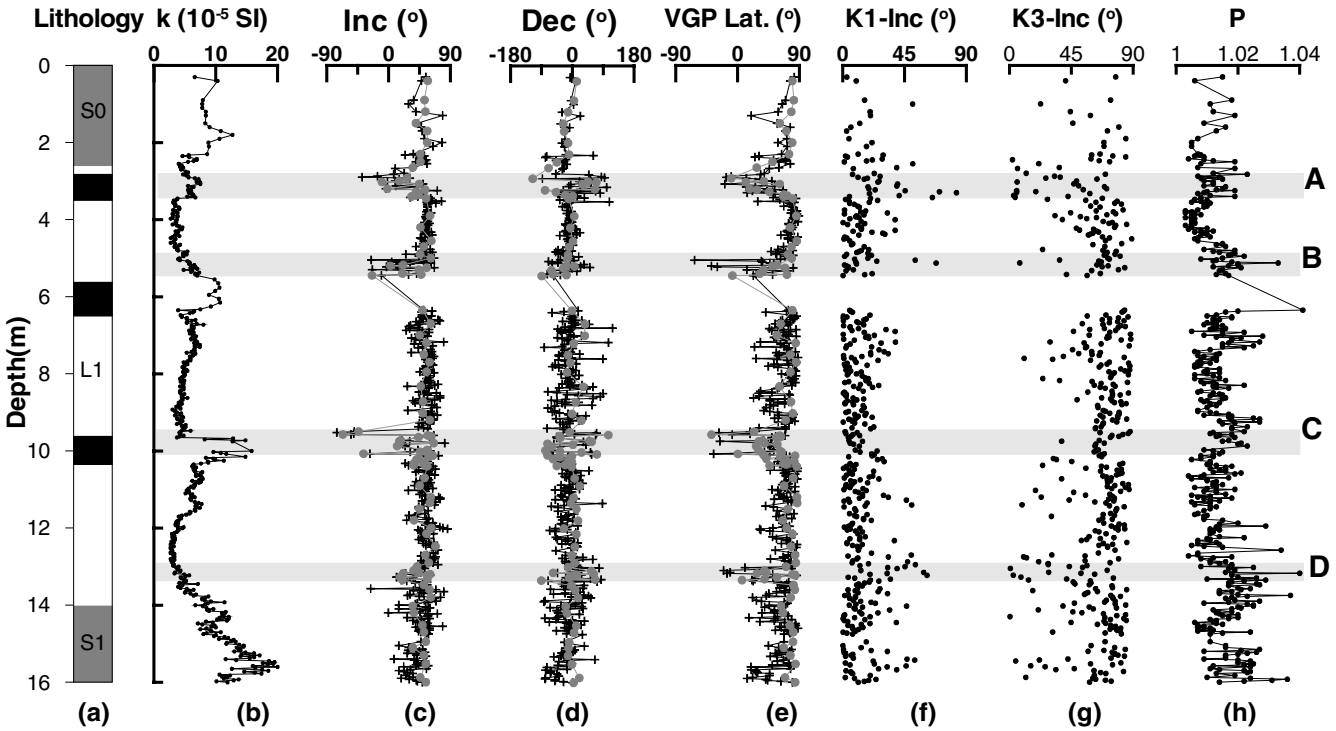


**Figure 5.** Stratigraphy (a) and depth plots of magnetic susceptibility (b), inclination (c), declination (d), palaeolatitude (e), K1-Inc (f), K3-Inc (g) and the degree of AMS. The horizontal grey bars associated with the letters (A–D) mark the four directional anomalies. The black crossbars and grey circles show AF and thermal demagnetization results, respectively.

have higher P values than loess units. This is mainly because the long-axes of the pedogenically produced SP/SD particles are also confined in the bedding planes, enhancing K1 more than K3. Our results show that the sand layers have a higher P than the loess units. But the overall P values are fairly low (<∼1.025–1.03), indicating that the effects of the wind strength of the winter monsoon at the eastern margin of the loess plateau are muted than at the central and northern loess plateau.

## 5 DISCUSSION

The Mono Lake (MLE) and Laschamp (LE) geomagnetic excursions are the two most useful palaeomagnetic time markers over the last glacial period. The two excursions have been globally documented over a wide range. For example, MLE has been found in lacustrine sediments from the Great Basin of western North America (Liddicoat & Coe 1979; Negrini *et al.* 1984; Liddicoat 1992), in marine sediments from the Atlantic and Arctic Oceans (Nowaczyk 1997; Nowaczyk & Knies 2000), and in wind-blown Chinese loess (Zhu *et al.* 1999). For LE, it has also been recorded in various media (Langereis *et al.* 1997; Zhu *et al.* 1999; Nowaczyk & Knies 2000). Moreover, the independence of these two excursions has been faithfully demonstrated by the coexistence of these two geomagnetic excursions at one profile from Chinese loess (Zhu *et al.* 1999) and from marine sediments (Nowaczyk & Knies 2000).

The age of LE was reported to be 40–35 ka (Hall & York 1978; Gillot *et al.* 1979), ∼44 ± 13.66 ka (Thouvney & Creer 1992), 46.8–37.4 ka (Zhu *et al.* 1999), ∼37–35 ka (Nowaczyk & Knies 2000), or ∼40–41 ka (Lund *et al.* 2005). For MLE, it mostly occurred at 27.1–26.0 ka (Zhu *et al.* 1999), 29.5–27.3 ka (Negrini *et al.* 1984) or 33.3–31.5 ka (Benson *et al.* 2003). The age discrepancies among these studies are probably due to different experiment methods and

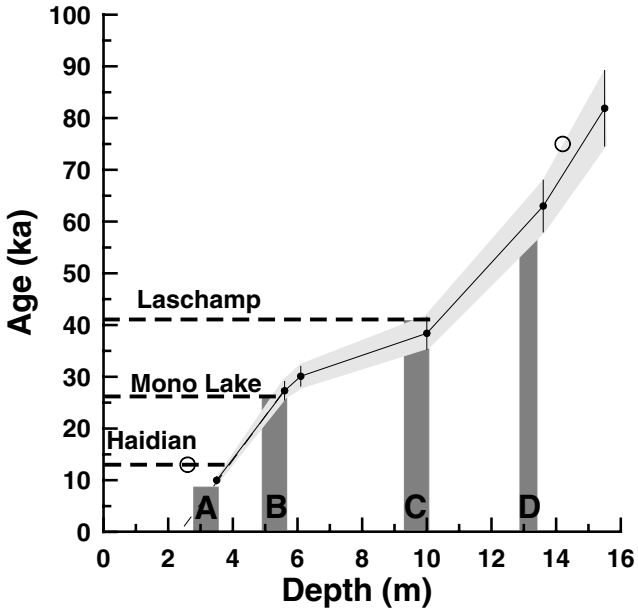


**Figure 6.** The correlation between the OSL ages (solid circles with error bars) and depth. The upper horizontal dashed lines mark the Laschamp and Mono Lake, and the Haidian excursions documented by Zhu *et al.* (1998c). The darker grey bars mark the four directional anomalies. The two open circles represent the pedostratigraphy age controls defined by the sharp changes in $\kappa_{fd}$ per cent in Fig. 2.

the inherent errors. Nevertheless, these ages are fairly consistent. In summary, the LE and MLE occur around 40 ka and 30 ka, respectively. Fig. 6 summarizes the depth–age model and the relevant geomagnetic events. The directional anomalies B and C could be

correlated to MLE and LE, respectively, based on this depth–age model.

Based on the OSL age controls, anomaly A is at ∼9 ka. However, if we assign the sharp boundary of $k_{fd}$ per cent at ∼2.5 m (Fig. 2c) as the boundary (∼12 ka) between MIS1 and MIS2, the age of anomaly A will be ∼13 ka. Zhu *et al.* (1998c) have even reported a geomagnetic excursion (∼14 ka) in the lake sediment from Haidian, Beijing, which is near the Datong section. It appears that anomaly A can be correlated to this Haidian counterpart. However, Fig. 5(c) shows that anomaly A, corresponding to the top sand layer, coincides with the K1-Inc anomaly. Because the AMS anomaly reflects the variation of depositional environments or disturbance of remanence directions after deposition, that is, the directional anomaly A is very sceptical. The same rationale can be applied to anomaly D (∼60 ka) as well as B, although the age of anomaly B coincides with that of MLE. So far, no equivalent excursion has been reported at this age. Therefore, the most reasonable interpretation is that this directional anomaly is also caused by depositional environment changes, suggested by the corresponding K1-Inc anomaly. In addition, it can be noted that K1-Inc is stable in horizontal plane while K3-Inc is relatively distorted (Figs 5f–h). This could be interpreted as fluvial currents and/or cryoturbation.

The NRM acquisition history of the Chinese loess is a complex process, which involves the effects of sedimentation rate, degree of pedogenesis, and post-depositional disturbance. Zhu *et al.* (1998b) systematically investigated the consistency of the Blake event over the Chinese loess plateau. They put forward:

(1) the western part of the loess plateau is relatively isolated from the strong dust storms. Moreover, the degree of pedogenesis is low. This has sufficiently minimized local erosion and redeposition and

(2) the northern margin of the loess plateau is near the desert and could have suffered much alteration (e.g. erosion and hiatus) than other regions.

The Laschamp event has been previously documented to be recorded in the Weinan profile, southern edge of the Chinese loess plateau (Zhu *et al.* 1999). However, the morphology for the magnetic field during the Laschamp event recorded in the Chinese loess does not resemble the records from the other studies (Lund *et al.* 1988). Our new results further demonstrate that interprofile comparison of the magnetic excursion recorded by the Chinese loess is also poor. Zhu *et al.* (1999) put forward that these differences are probably caused by the lock-in effects, accumulation rate, smoothing realignment, etc. The inherent non-dipole features of the magnetic excursion could be another important reason (Merrill & McFadden 2005). They concluded that it is questionable to directly correlate two excursion records separated by angular distances more than 45° on the Earth's surface. Therefore, this study does not attempt to compare our results with the other records, specially in terms of the morphology of magnetic field during excursions. Nevertheless, the age consistence of the Laschamp event recorded by different loess profiles demonstrates that Chinese loess can record at least the event.

The Datong profile is located at the northeastern margin of the loess plateau, where the effects of pedogenesis and depositional environment variations are supposed to be high. However, these effects have been minimized by the high sedimentation rate for some periods. For example, the overall sedimentation rate of this profile is about two times higher than that of the profiles at the central loess plateau. This is mainly because the Datong Basin is a relatively closed system. The detrital material from the local regions is abundant, and can be easily transported and deposited at this site. Furthermore, the $\kappa_{fd}$ per cent for the loess unit L1 is only several percent, indicating that the effect of pedogenesis is also not high. Therefore, the loess unit at the Datong profile is suitable to record short-term palaeomagnetic signals, especially during some periods with high sedimentation rate and relatively low degree of pedogenesis. However, depositional environment changes can also yield sceptical directional anomalies, but which can be easily identified by the corresponding abnormal AMS behaviour.

## 6 CONCLUSIONS

To confidently evaluate the fidelity of the palaeomagnetic signals recorded by the Chinese loess, records from different regions at the Chinese loess plateau are necessary. The results from the northeastern margin of the loess plateau since the end of the last interglacial period record four palaeodirectional anomalies (A–D). However, anomalies A, B and D coincide with the corresponding K1-Inc anomalies, indicating that they are most probably caused by depositional environment variations. In contrast, anomaly C occurs at ∼40 ka with relatively normal AMS. This directional anomaly is believed to be the true geomagnetic signal, which can be correlated to the Laschamp excursion. These results further demonstrate that loess units can record short-term features of the Earth's magnetic field. Nevertheless, cautions have to be made to rule out the artefacts caused by depositional environment variations.

## ACKNOWLEDGMENTS

We thank Dr C. Shi for carrying out field work and part of the lab work. We also thank Profs F. Heller, M. E. Evans and C. G. Langereis (editor) for constructive suggestions on this manuscript. This study was supported by NSFC (grant nos. 40221402 and 40325011).

## REFERENCES

Benson, L., Liddicoat, J., Smoot, J., Sarna-Wojcicki, A., Negrini, R. & Lund, S., 2003. Age of the Mono Lake excursion and associated tephra, *Quat. Sci. Rev.,* **22,** 135–140.

Deng, C., Zhu, R., Verosub, K.L., Singer, M.J. & Vidic, N.J., 2004. Mineral magnetic properties of loess/paleosol couplets of the central loess plateau of China over the last 1.2 Myr, *J. geophys. Res.,* **109,** B01103, doi: 10.1029/2003JB002532.

Dunlop, D.J., Xu, S. & Heider F., 2004. Alternating field demagnetization, single-domain-like memory, and the Lowrie-Fuller test of multidomain magnetite grains (0.6–356 mm), *J. geophys. Res.,* **109,** B07102, doi:10.1029/2004JB003006.

Evans, M.E. & Heller, F., 2001. Magnetism of loess/paleosol sequences: recent developments, *Earth Sci. Rev.,* **54,** 129–144.

Fang, X.M. et al, 1997. A record of the Blake Event during the last interglacial Paleosol in the western Loess Plateau of China, *Earth planet. Sci. Lett.,* **146,** 73–82.

Gillot P.Y., Labeyrie, J., Laj, C., Valladas, G., Guérin, G., Poupeau, G. & Delibrias, G., 1979. Age of the Laschamp paleomagnetic excursion revisited, *Earth planet. Sci. Lett.,* **140,** 444–450.

Heller, F. & Liu, T.S., 1982. Magnetostratigraphical dating of loess deposits in China, *Nature,* **300,** 431–433.

Heller, F. & Evans, M.E., 1995. Loess magnetism, *Rev. Geophys.,* **33,** 211–240.

Hall, C.M. & York, D., 1978. K-Ar and $^{40}Ar/^{39}Ar$ age of the Laschamp geomagnetic polarity reversal, *Nature,* **140,** 462–464.

Huntley, D.J., Godfrey-Smith, D.I. & Thewalt, M.L.W., 1985. Optical dating of sediments, *Nature,* **313,** 105–107.

Hütt, G., Jaek, I. & Tchonka, J., 1988. Optical dating: K-feldspars optical response stimulation spectra, *Quat. Sci. Rev.,* **7,** 381–385.

Jelinek, V., 1977. The statistical theory of measuring anisotropy of magnetic susceptibility of rocks and its application, Brno, *Geophysika*, 1–88.

Kirschvink, J.L., 1980. The least-squares line and plane and analysis of paleomagnetic data, *Geophys. J. R. Astron. Soc.,* **62,** 699–718.

Lang, A., Lindauer, S., Kuhn, R. & Wagner, G.A., 1996. Procedures used for optically and infrared stimulated luminescence dating of sediments in Heidelberg, *Ancient TL,* **14,** 7–11.

Langereis, C.G., Dekkers, M.J., Lange, G.J., Paterne, M. & Van Santvoort, P.J.M., 1997. Magnetostratigraphy and astronomical calibration of the last 1.1 Myr from eastern Mediterranean piston core and dating of short events in the Brunhes, *Geophys. J. Int.,* **129,** 75–94.

Liddicoat, J.C. & Coe, R.S., 1979. Mono Lake geomagnetic excursion, *J. geophys. Res.,* **84,** 261–271.

Liddicoat, J.C., 1992. Mono Lake excursion in Mono Basin, California, and at Carson Sink and Pyramid Lake, Nevada, *Geophys. J. Int.,* **108,** 442–452.

Liu, Q., Banerjee, S.K., Jackson, M.J., Chen, F., Pan, Y. & Zhu, R., 2003. An integrated study of the grain-size-dependent magnetic mineralogy of the Chinese loess/paleosol and its environmental significance, *J. geophys. Res.,* **108**(B9), 2437, doi:10.1029/2002JB002264.

Liu, Q.S., Deng, C.L., Yu, Y., Torrent, J., Jackson, M.J., Banerjee, S.K. & Zhu, R.X., 2005a. Temperature dependence of magnetic susceptibility: implications for pedogenesis of Chinese loess/palaeosols, *Geophys. J. Int.,* **161,** 102–112.

Liu, Q.S., Yu, Y.J., Deng, C.L., Pan, Y.X. & Zhu, R.X., 2005b. Enhancing weak magnetic fabrics using field-impressed anisotropy: application to the Chinese loess, *Geophys. J. Int.,* **162,** 381–389.

Liu, T.S., 1958. Preliminary investigation on the loess of Shanxi and Shaanxi Provinces in the middle reaches of the Huanghe River, *Quarter. Sinica,* **1,** 255–257 (in Chinese).

Liu, X., Xu, T. & Liu, T., 1988. The Chinese loess in Xifeng. II. A study of anisotropy of magnetic susceptibility of loess from Xifeng, *Geophys. J. Int.,* **92,** 349–353.

Lund, S.P., Schwartz, M., Keigwin, L. & Johnson, T., 2005. Deep-sea sediment records of the Laschamp geomagnetic field excursion (~41,000 calendar years before present), *J. geophys. Res.,* **110,** B04101, doi: 10.1029/2003JB002943.

Maher, B.A., 1998, Magnetic properties of modern soils and Quaternary loessic paleosols: paleoclimatic implications, *Palaeogeogr., Palaeoclimatol., Palaeoecol.,* **137,** 25–54.

Merrill, R.T. & McFadden, P.L., 2005. The use of magnetic field excursions in stratigraphy, *Quat. Res.,* **63,** 232–237.

Negrini, R.M., Davis, J.O. & Verosub, K.L., 1984. Mono Lake geomagnetic excursion found at Summer Lake, Oregon, *Geology,* **12,** 464–643.

Nowaczyk, N.R., 1997. High-resolution magnetostratigraphy of four sediment cores from the Greenland Sea—II. Rock magnetic and relative palaeointensity data, *Geophys. J. Int.,* **131,** 325–334.

Nowaczyk, N.R. & Knies, J., 2000. Magnetostratigraphic results from the eastern Arctic Ocean: AMS $^{14}$C ages and relative palaeointensity data of the Mono Lake and Laschamp geomagnetic reversal excursions, *Geophys. J. Int.,* **140,** 185–19.

Pan, Y.X., Zhu, R.X., Liu, Q.S., Guo, B., Yue, L.P. & Wu, H.N., 2002. Paleomagnetic episodes of the last 1.2 Myr recorded in Chinese loess, *Geophys. Res. Lett.,* **29** (8), doi: 10.1029/2001GL014024.

Rolph, T.C., Shaw, J., Derbyshire, E. & Wang, J.T., 1989. A detailed geomagnetic record from Chinese loess, *Phys. Earth planet. Inter.,* **56,** 151–164.

Spassov, S., Heller, F., Evans, M.E., Yue, L.P. & von Dobeneck, T., 2003. A lock-in model for the complex Matuyama-Brunhes boundary record of the loess/palaeosol sequence at Lingtai (central Chinese Loess Plateau), *Geophys. J. Int.,* **155,** 350–366.

Sun, D., Shaw, J., An, Z.& Rolph, T.C, 1993. Matuyama/Brunhes (M/B) transition recorded in Chinese loess, *J. Geomag. Geoelec.,* **45,** 319–330.

Thouvney, N. & Creer, K.M., 1992. On the brevity of the Laschamp excursion, *Bull. Soc. Geol. Fr.,* **163,** 771–780.

Yang, T., Hyodo, M., Yang, Z. & Fu, J., 2004. Evidence for the Kamikatsura and Santa Rosa excursions recorded in eolian deposits from the southern Chinese Loess Plateau, *J. geophys. Res.,* **109,** B12105, doi: 10.1029/2004JB002966.

Zheng, H.B., Rolph, T., Shaw, J. & An, Z.S., 1995. A detailed palaeomagnetic record for the last interglacial period, *Earth planet. Sci. Lett.,* **133,** 339–351.

Zhou, L.P. & Shackleton, N.J., 1999. Misleading positions of geomagnetic reversal boundaries in Eurasian loess and implications for correlation between continental and marine sedimentary sequences, *Earth planet. Sci. Lett.,* **168,** 117–130.

Zhu, R., Ding, Z., Wu, H., Huang, B. & Jiang, L., 1993. Details of magnetic polarity transition recorded in Chinese loess, *J. Geomag. Geoelec.,* **45,** 289–299.

Zhu, R.X., Laj, C. & Mazaud, A., 1994a. The Matuyama-Brunches and upper Jaramillo transitions recorded in a loess section at Weinan, north-central China, *Earth planet. Sci. Lett.,* **125,** 143–158.

Zhu, R.X., Zhou, L.P., Laj, C., Mazaud, A. & Ding, Z.L., 1994b. The Blake geomagnetic polarity episode recorded in Chinese loess, *Geophys. Res. Lett.,* **21,** 697–700.

Zhu, R.X., Pan, Y.X., Guo, B. & Liu, Q.S., 1998a. A recording phase lag between ocean and continent climate changes constrained by the Matuyama/Brunhes polarity boundary, *Chin. Sci. Bull.,* **43,** 1593–1598.

Zhu, R.X., Coe, R.S., Bin, G., Robert, A. & Zhao, X.X., 1998b. Inconsistent palaeomagnetic recording of the Blake Event in Chinese loess related to sedimentary environment, *Geophys. J. Int.,* **134,** 867–875.

Zhu, R.X., Coe, R.S. & Zhao, X.X., 1998c. Sedimentary record of two geomagnetic excursions within the last 15 000 years in Beijing, China, *J. geophys. Res.,* **103,** 30 323–30 333.

Zhu, R.X., Pan, Y.X. & Liu, Q.S., 1999. Geomagnetic excursions recorded in Chinese loess in the last 70 000 yr, *Geophys. Res. Lett.,* **26,** 505–508.

Zhu, R.X., Liu, Q.S. & Jackson, M.J., 2004. Paleoenvironmental significance of the magnetic fabrics in the Chinese loess-paleosols since the last interglacial (<130 ka), *Earth planet. Sci. Lett.,* **221,** 55–69.

Zijderveld, J.A.C., 1967. Demagnetization of rocks: analysis of results, in *Methods in Paleomagnetism*, pp. 254–286, eds Collinson, D., Creer, K. & Runcorn, S., Elsevier, New York.